Osmotic Flow Effects on the Dialysis Escape Curves of Solutes

Dien-Feng Shieh, Jan Feijen,[1] and Donald J. Lyman

Department of Materials Science and Engineering, University of Utah, Salt Lake City, UT 84112

While dialysis has been widely used as a separation technique for a long time, Craig and his coworkers (*1, 2*) recently developed it as a simple and convenient method to characterize a variety of biochemical solutes. This characterization is based on the shape of the escape curves of the solutes during aqueous thin-film dialysis. With this thin-film technique, the dialyzing solution (about 0.6 ml) can be uniformly distributed over 40–50 cm^2 of membrane area. The outside solution (10 to 20 times the volume of the dialyzing solution) is replaced periodically with fresh solvent and the concentration of the dialyzed solute measured at that time. A plot of percentage of solute remaining vs. time on a semilog scale is called the escape curve. Different shapes can be observed for different solute, solvent, and membrane combinations. The systems with straight escape curves were described as "ideal"; nonlinearity in the escape curves was explained in terms of impurity, association, or aggregation of the solutes studied (*3*).

Recently, Stewart et al. (*4*) carried out computer calculations, based on first-order kinetic models, to show how solute impurity, association, or aggregation could cause the escape curves to deviate from linearity. While no proof was mentioned about the kinetic models used in their calculations, deviation from linearity can still be observed even with pure homogeneous solutes that do not associate (*1*).

Though many factors affect the observed shape of the escape curves, one phenomenon, i.e., osmotic flow, although well known itself, has been neglected. In this paper, we would like to stress its importance in affecting the shape of the escape curves. Computer calculations in terms of three phenomenal parameters—permeability coefficient, filtration coefficient, and reflection coefficient—were used to illustrate the effects. The calculations are qualitatively confirmed by experimental results reported for the thin film dialysis measurements.

THEORY AND CALCULATIONS

A general dialysis system can be described as consisting of two compartments with volumes V_1 and V_2 separated by a membrane with effective area S. The concentrations of the solutes in compartments 1 and 2 are designated as C_{S_1} and C_{S_2}. The mass flux J_S through the membrane is given by

$$J_S = U(C_{S_1} - C_{S_2}) \tag{1}$$

where U is defined as the overall permeability. From the mass balance, we obtain

$$\frac{d(V_1 C_{S_1})}{dt} = -J_S S \tag{2}$$

If $V_2 \gg V_1$ and $C_{S_2} \ll C_{S_1}$, which are the experimental conditions reached in thin film dialysis, it can be shown that

$$\ln \frac{C_{S_1}}{C_{S_1}^{\circ}} = -\frac{US}{V_1} t \tag{3}$$

where $C_{S_1}^{\circ} = C_{S_1}$ $(t = 0)$.

Plotting $\ln C_{S_1}/C_{S_1}^{\circ}$ as a function of time leads to a linear plot only when $(US)/V_1$ is constant. Depending on the dialysis system used, U and S are approximately constant, but V_1 can change significantly as a result of osmotic flow. Furthermore, although the outside concentration C_{S_2} can be kept nearly zero by frequent replacement of the solvent in compartment 2, a more accurate description of the transport phenomena in the case of longer time intervals between the change of solvent $(t_n - t_{n-1})$ is given by

$$\ln \left[\left(1 + \frac{V_1}{V_2}\right) \frac{(C_{S_1})_n}{(C_{S_1})_{n-1}} - \frac{V_1}{V_2} \right] = -US \left(\frac{1}{V_1} + \frac{1}{V_2}\right) (t_n - t_{n-1}) \tag{4}$$

where $(C_{S_1})_n$ is the concentration in compartment 1 at time t_n and $(C_{S_1})_{n-1}$ is the concentration at time t_{n-1}. If $(t_n - t_{n-1})$ is small, Equation 3 is the same as Equation 4. When $(t_n - t_{n-1})$ is large, Equation 4 should be used to describe the experimental system. It should be noted here that the derivation of Equation 4 is based on the assumption of constant V_1 and V_2 during the interval $(t_n - t_{n-1})$. However, as a result of osmotic flow, V_1 will increase as given by

$$V_1(t_n) = V_1(t_{n-1}) + J_V S(t_n - t_{n-1}) \tag{5}$$

where J_V is the volumetric flow rate. When $t = 0$, $V_1 = V_1^{\circ}$.

In the case where V_2 is much larger than V_1, V_2 can be considered reasonably constant.

In order to describe this osmotic flow, we used general phenomenal equations derived from the irreversible thermodynamic theory. Three experimentally measurable parameters, the filtration coefficient L_p, the reflection coefficient σ, and the permeability coefficient ω can be used to describe the phenomena (*5*).

The volumetric flow rate J_V is given by

$$J_V = L_p(\Delta p - \sigma \Delta \pi) \tag{6}$$

The parameter σ can vary from zero for solutes that have the same permeability as water, to one for solutes that are completely rejected by the membrane. The hydrostatic pressure difference is given by Δp whereas the theoretical osmotic pressure difference $\Delta \pi$ equals $RT\Delta C_S/M_n$. (ΔC_S is the mean concentration difference across the membrane.)

The net solute flux across the membrane J_S is given by:

$$J_S = \bar{C}_S(1 - \sigma)J_V + \omega \Delta \pi \tag{7}$$

where $\bar{C}_S = (C_{S_1} - C_{S_2})/(\ln C_{S_1}/C_{S_2})$. For very small concentration differences, $\bar{C}_S \simeq (C_{S_1} + C_{S_2})/2$.

Combining Equations 1, 6, and 7, it can be shown that

$$U = [\omega - \bar{C}_S(1 - \sigma)\sigma L_p]RT \text{ for } \Delta p = 0 \tag{8}$$

[1] Present address, Department of Chemical Technology, T.H.T., Enschede, The Netherlands.

Equations 4, 5, 6, and 8 were simultaneously solved using a digital computer. V_1 was kept constant in Equation 4 during $t_{n-1} \leq t < t_n$, and at t_n, V_1 increased as described by Equation 5. The percentage of solutes remaining in compartment 1, i.e., $[(C_{S_1})_n\ (V_1)_n]/(C_{S_1}{}^\circ V_1{}^\circ) \times 100\%$, as a function of time t_n, was then obtained for different sets of ω, σ, and L_p, and for different dialyzers.

RESULTS AND DISCUSSION

A typical calculation result for the "thin-film" dialysis system (i.e., $V_1{}^\circ$ = 0.6 ml, V_2 = 9 ml, and S = 45 cm^2) is shown in Figure 1. Depending on the values of the filtration coefficient L_p, permeability coefficient ω and reflection coefficient σ, the escape curves are either straight lines or upward curves with one or two breaking points. All the values chosen for ω, σ, and L_p are within a reasonable range (p 123, Ref. 5) and the volume change inside the cell is all less than 1.0 ml. For the systems with high ω and low σ, the osmotic flow would be small and the escape curves are straight. As σ becomes larger or ω smaller, for example, for higher molecular weight compounds, the osmotic flow would be much more pronounced, and deviation from linearity would obviously be observed.

The filtration coefficient L_p represents a kind of mechanical filtration capacity of the membrane and is defined as in Equation 6. If a pressure difference across a membrane is maintained, and even though the tonicity is the same on both sides of the membrane, there will exist a volume flow J_V, which is a linear function of Δp. The proportionality coefficient relating to J_V to Δp is L_p (5). It has the character of a mobility and represents the velocity of fluid per unit pressure difference. Experimentally, L_p can be obtained by observing the volumetric flow change as Δp applied when the solution concentrations on both sides are equal. The solute permeability coefficient ω is the intrinsic mobility of a solute through the membrane or the permeability of a solute when the solvent flow is negligible. As can be seen from Equation 7, when $J_V \simeq 0$, $J_S = \omega\Delta\pi$. Practically, ideal semipermeable membrane rarely exists. More often the membrane is slightly permeable to all solutes. It has been convenient to define a new coefficient called the reflection coefficient or the Staverman factor σ, $\sigma = -L_{pd}/L_p$ (5). For ideal semipermeable membrane, σ = 1.0; for a coarse, completely nonselective membrane σ is zero. It can be said that the reflection coefficient is a measure of the semipermeability of the membrane to a particular solute. When σ is larger, ω should be smaller, and these two coefficients are not independent (5). As we can see from Equation 6, σ can be determined from the ratio of the volume flow, J_V, to the product of the filtration coefficient, L_p, and the osmotic pressure difference, $\Delta\pi$, when the applied pressure, Δp is zero. However, experimentally it is often easier to measure the volume flow when a hydrostatic pressure is applied across the membrane. An example of practical experiment technique and apparatus to measure all these three coefficients can be found in Reference 7. Sometimes, it might be more convenient to measure the actual volume change of V_1 and adjust it in studying directly the escape curves obtained.

In the actual sense, the three parameters used to describe the dialysis system probably would not be constant in the whole experimental period of obtaining the dialysis escaping curves. However, as shown in Figure 1, with some chosen reasonable values of the coefficients, the upcurving effects of the osmotic flow can be illustrated. Similar to Figure 1, with the thin-film dialysis system, almost all the escape curves reported for a homologous series of sugars show an upward curvature (6). Even without going to complicated calculations as described above, the up-curving effect can be obviously seen in Equation 3. As V_1 increases, due to osmotic flow, $(US)/V_1$ decreases, which means that the negative slope of the curve ln $C_{S_1}/C_{S_1}{}^\circ$ vs. t becomes smaller and smaller and the escape curves go upward as time goes.

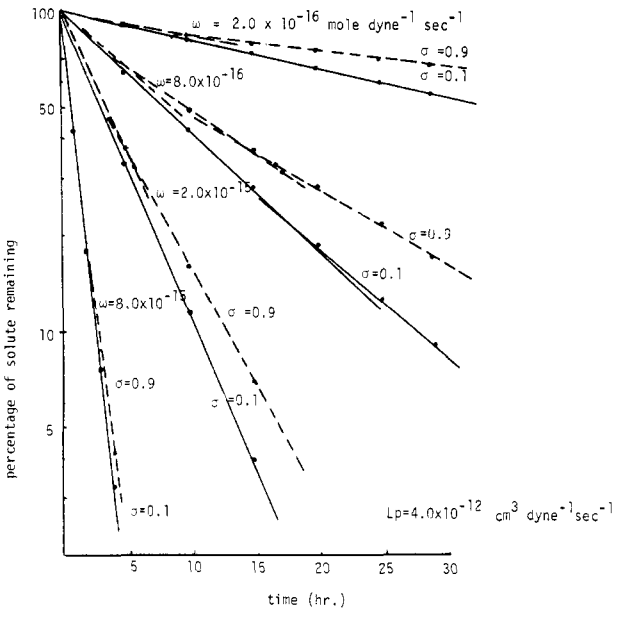

Figure 1. Calculated escape curves for dialyzer with V_1 (t = 0) = 0.6 ml, V_2 = 9 ml and effective membrane area S = 45 cm^2

Since the total osmotic flow rate is directly proportional to the membrane area available, the volume change in V_1 would be much pronounced for the system with a high ratio of membrane area to V_1, like the "thin-film" dialysis system. When this kind of system is used to characterize a variety of naturally occuring solutes, the dilution effects were obviously observed and, for certain proteins, the increase in V_1 was reported as much larger than 50% (1).

In a dialysis system where the ratio of membrane area to the cell volume is much smaller than that in thin film dialysis system, the osmotic effect would be much less severe, and little attention was paid to its effect on the shape of escape curves.

In applying the dialysis technique to characterize the relatively high molecular weight compounds, even when experimentally a straight escape curve is obtained, no definite conclusions could be made with respect to the "ideality" of the compounds in solution. This is because the downward curving effect inherently caused by solute aggregation (4) could be masked by upward curving effects of osmotic flow on the escape curves.

In the present paper, we have illustrated the effect of osmotic flow on the up-curving of the escape curves using the three parameters L_p, ω, and σ and compared some experimental results available. With the knowledge of the effect of this osmotic flow on the escape curves, the much more complicated properties such as aggregation, association, etc. of biochemical compounds in solution could then be more clearly characterized with the dialysis technique.

LITERATURE CITED

(1) L. D. Craig, T. P. King, and A. Stracher, *J. Am. Chem. Soc.*, **79**, 3729 (1957).
(2) L. C. Craig, "Membrane Science and Technology," J. E. Flinn, Ed., Plenum, New York, 1970, p 1.
(3) M. A. Ruttenberg, T. P. King, and L. C. Craig, *Biochemistry*, **5**, 2857 (1966).
(4) K. K. Stewart, L. C. Craig, and R. C. Williams, Jr., *Anal. Chem.*, **42**, 1252 (1970).

(5) A. Katchalsky and P. F. Curran, "Nonequilibrium Thermodynamics in Biophysics," Harvard University Press, Boston, MA, 1965.
(6) L. C. Craig and A. O. Pulley, *Biochemistry*, **1**, 89 (1962).
(7) B. K. Fritzinger, S. K. Brauman, and D. J. Lyman, *J. Biomed. Mater. Res.*, **5**, 3 (1971).

RECEIVED for review September 3, 1974. Accepted February 3, 1975. Significant portions of this paper were presented at the Symposium on Membranes in Separation Processes, Case Western Reserve University, Cleveland, OH, May 8–10, 1973. This work was supported under National Science Foundation Grant No. GH-38996X.

Description of the Thermal Energy Analyzer (TEA) for Trace Determination of Volatile and Nonvolatile *N*-Nitroso Compounds

David H. Fine,[1] Firooz Rufeh, David Lieb, and David P. Rounbehler

Thermo Electron Corporation, 85 First Avenue, Waltham, MA 02154

Many *N*-nitroso compounds are known to be carcinogenic (*1, 2*), and there is much concern about their possible widespread occurrence in the environment (*3*). Analytical methods, sensitive at the μg/kg level in the original material, are available for the more volatile *N*-nitrosamines (*4, 5*). The procedures involve concentration and cleanup by distillation and/or extraction, followed by separation by gas–liquid chromatography (GLC) and detection by either the Coulson electrolytic conductivity or the alkali flame ionization detectors (*6*). Because they are nonspecific to *N*-nitroso compounds, the GLC detectors are useful for screening purposes only; confirmation by GLC–mass spectrometry is still mandatory (*7, 8*). Judging from the wide variety of complex secondary amines occurring in nature, a large group of naturally-occurring high molecular weight *N*-nitroso compounds is to be expected. As a result of their high molecular weight, they would be nonvolatile, and not amenable to GLC analysis or to cleanup by steam or vacuum distillation. For this reason, adequate methods are not yet available for the analysis of nonvolatile *N*-nitroso compounds.

A new detection technique, called the Thermal Energy Analyzer (TEA), which is both highly sensitive and highly selective to all *N*-nitroso compounds, has been reported recently (*9, 10*). We report here on a practical TEA system which may also be used as a detector for gas–liquid chromatography (*11*). The scope and limitations of the technique are described in terms of sensitivity to different *N*-nitroso compounds, and quantitative limitations are placed on selectivity and performance. The detector as described here is an analytical tool capable of selectively detecting sub-μg/kg amounts of *N*-nitroso compounds in complex biological materials and foodstuffs. The fundamental principles and the theoretical concepts underlying the technique are described elsewhere (*12*).

EXPERIMENTAL

Description of the TEA. A dilute solution containing the *N*-nitroso compound is injected directly into a catalytic pyrolyzer. The pyrolyzer inlet is constructed in a manner similar to a gas chromatograph injection port, with provision for preheated carrier gas, a septum, and electrical heaters for maintaining the temperature in excess of 275 °C. A schematic of the TEA is shown in Figure 1. At the same time as vaporizing the solvent, the *N*-nitroso compound is decomposed into a nitrosyl radical and an organic radical. The organic fragment either decomposes further (*13, 14*) or rearranges to give a stable product, which together with the solvent vapor and the nitrosyl radical are swept through a capillary restriction into an evacuated reaction chamber, maintained at reduced pressure by a 140 l./min rotary vacuum pump. Ozone, formed by high voltage electric discharge (7500 volts across a 1-mm glass dielectric) in oxygen, also enters the reaction chamber through a capillary restriction, where it reacts with the nitrosyl radical yielding electronically excited NO_2*. The excited NO_2* rapidly decays back to its ground state, with the emission of light in the near infrared region of the spectrum. The intensity of the emission is detected by means of a S-20 photomultiplier tube (RCA 3000 CN), in conjunction with a red optical filter (Corning CS2-60). The photomultiplier response is amplified electronically and displayed on a chart recorder. In order to minimize photomultiplier tube dark current, the tube is kept in a shielded housing maintained at −20 °C.

Chemicals. Standard solutions containing approximately 1 μg *N*-nitroso compound per ml solvent were made up gravimetrically. Depending on the solubility and stability of the particular *N*-nitroso compound, either ethanol or dichloromethane was used as the solvent.

Compounds for interference testing were chosen for one of several reasons: because of their structure and the presence of either NO_2 or NO functional groups; because of their great abundance in many foodstuffs and biological materials; because they may be formed in the TEA by rearrangement and pyrolysis of parent species; or because of their frequent use as solvents either in gas chromatography or in high performance liquid chromatography. A stock solution containing 0.1 μg of *N*-nitrosodiphenylamine per ml of dichloromethane was prepared. Using the stock solution as the solvent, 1% solutions of the compounds to be tested were made up gravimetrically. If the compound was not soluble in dichloromethane, another solvent was used, both for the standard solution and also for the test solution.

All the solvents, the *N*-nitroso compounds, and the potential interferences were used as received, without further purification.

Procedure. As in gas chromatography, 1- to 10-μl liquid samples were introduced, by means of a hypodermic needle, directly into the flash vaporization chamber of the TEA.

RESULTS

The integrated TEA response to approximately 1 μg/ml solutions of twelve different *N*-nitroso compounds in ethanol is shown in Table I.

Calibration curves for five *N*-nitroso compounds of different chemical structure (*N*-nitrosodimethylamine, *N*-nitroso-*N*-ethylaniline, 9-nitrosocarbazole, *N*-nitroso-*N*-methyl urethane, and *N*-methyl-*N*-nitroso-*N*-nitroguanidine) are shown in Figure 2.

Table II is a listing of those compounds which gave no detectable response on the TEA (a *N*-nitroso compound to interference ratio of greater than 10,000 to 1). No compounds have been found which give a negative response. Table III lists those compounds for which a positive response was observed. The magnitude of the response is re-

[1] Author to whom correspondence should be addressed.